International Journal of Applied Mathematics and Engineering Sciences
Vol. 2 No. 2 (December, 2017)

CHANGING FLOOD RISKS IN ESTUARIES DUE TO GLOBAL CLIMATE CHANGE: FORECASTS FROM OBSERVATIONS, THEORY AND MODELS

Andrew Lane & David Prandle

ABSTRACT: Rising sea levels and enhanced storminess, resulting from Global Climate Change, pose major threats to the viability of estuaries worldwide. While numerical models can accurately simulate changes in estuarine responses for tides and surges, they cannot reliably predict related bathymetric evolution and its effects on these responses. Here, it is shown how observations, theory and model studies can be used to understand these evolving interactions between tidal dynamics, sediment regime, and bathymetry. Concentrating on the Mersey Estuary, the capabilities of a fine-resolution 3-D model are assessed against the perspective of historical changes in tides, sediments and estuarine bathymetries. New theoretical frameworks can be used to interpret ensemble simulations of parameter sensitivities. The methodologies should be applicable across a broad range of estuaries. Generally, relatively small and gradual changes are expected in most estuaries. However, conditions which might produce major abrupt changes are identified.

1. INTRODUCTION

By 2050, Global Climate Change (GCC) could significantly change mean sea levels, storminess, river flows and sediment supply in estuaries (IPCC, 2001). The tidal and surge response within any estuary will be further modified by accompanying natural morphological (post-Holocene) adjustments alongside impacts from past and present 'interventions'.

There is an urgent need to develop models that can indicate the possible nature, extent and rate of these morphological changes. Given specified bathymetry and surficial sediment distribution, numerical models can accurately reproduce water levels and currents. However, the corresponding simulation of sediment regimes is more problematic. It involves much wider spectral scales with net fluxes generally determined by non-linear coupling of residual and tidal constituents associated with both flow and sediment suspension. On longer time scales, sediment regimes are also sensitive to varying patterns of flora and fauna. Future forecasts must encapsulate a wide range of possible outcomes, i.e., provide an ensemble of predictions. The associated range of likely evolving morphologies widens sharply for extended forecast periods.

Morphological adjustment is generally slow, e.g., deposition per tide of a depth-mean concentration of 100 mg l^{-1} in 10 m water depth amounts to about 0.35 mm, or 25 cm per year. In reality, 'capture rates' (upstream deposition as a proportion of the net tidal inflow of suspended sediments) are typically only a few percent. Thus simulations need to extend over decades to embrace representative forcing cycles.

While the focus here is on the Mersey (UK), the methodologies should be broadly applicable across estuaries of varying sizes, shapes and morphological types. Subsequent Sections describe three approaches, namely: (i) analyses of historic data, (ii) new theories relating estuarine bathymetry to tides, river flow and sediment supply and (iii) 3-D numerical model simulations.

2. THE MERSEY ESTUARY

The Mersey is a macro-tidal estuary with extensive industrial and commercial activity. The estuary has been widely studied because of its vital role in transport (in particular shipping), and the designation of parts of the inner estuary basin as nature reserves and 'Sites of Special Scientific Interest'. Historically, the Mersey has

been seriously polluted by industrial discharges and adjacent sea dumping. A comprehensive programme to improve water quality is presently being undertaken.

The Mersey is a useful test bed for developing and evaluating estuarine tools. It has large tides, strong mixing, little influence of river flows and, a good observational data set including detailed sequences of bathymetry.

Tidal ranges in the Mersey vary from 4 to 10 m over the extremes of the spring-neap cycle (Table 1). The Narrows at the mouth of the 45 km-long estuary is approximately 1.5 km wide with a mean depth (below chart datum) of 15 m (Figure 1), and tidal currents through this section can exceed 2 m s^{-1}. Further upstream in the inner estuary basin, the width can be as much as 5 km, and extensive areas are exposed at low water. Freshwater flow into the estuary, Q, varies from 25 to 300 m^3 s^{-1} with a mean 'flow ratio' ($Q \times 12.42$ hr)/volume between high and low water) of approximately 0.01. Flow ratios of less than 0.1 usually indicate well-mixed conditions, though in certain sections during part of the tidal cycle, the Mersey is only partially mixed.

Table 1
Historical Changes in Mean Sea Level and Tidal Constituents in the Mersey. Amplitudes in metres, phases in degrees. Z_0 represents mean sea level above Ordnance Datum Newlyn

Location/	Z_0	M_2		S_2		M_4		M_4/M_2	$2M_2–M_4$
Year		*ampl.*	*phase*	*ampl.*	*phase*	*ampl.*	*phase*	*%*	
New Brighton									
1971	0.130	3.060	318.8°	0.998	3.7°	0.231	198.5°	7.54	79.1°
Gladstone Lock									
1965	0.250	3.078	321.6°	1.000	4.6°	0.219	201.9°	7.12	81.3°
1991	0.255	3.050	321.2°	0.981	6.1°	0.247	203.9°	8.10	78.5°
1991–93 (3 years)	0.271	3.042	321.2°	0.975	5.8°	0.244	203.1°	8.02	79.3°
Alfred Lock									
1963	0.194	3.120	324.1°	1.012	8.1°	0.234	214.5°	7.50	73.7°
1964	0.157	3.119	323.9°	1.007	7.9°	0.230	217.3°	7.37	70.5°
1968 (7 months)	0.258	3.171	323.6°	1.028	7.4°	0.216	213.6°	6.81	73.6°
1990	0.241	3.151	323.6°	1.020	8.8°	0.220	217.8°	6.98	69.4°
Princes Pier									
1918	0.100	3.076	326.9°	0.986	11.6°	–	–	–	–
1920	0.144	3.065	326.4°	0.980	11.8°	–	–	–	–
1922	–	3.068	326.6°	0.974	11.9°	–	–	–	–
1924	0.179	3.025	325.6°	0.950	9.9°	0.229	217.1°	7.57	74.1°
1930	0.154	3.090	325.4°	1.003	10.4°	0.224	222.4°	7.25	68.4°
1964	0.169	3.108	323.2°	1.005	7.5°	0.231	215.4°	7.43	71.0°
1963–81 (18.6 years)	0.208	3.121	323.5°	1.008	7.9°	0.221	214.2°	7.08	72.8°
Eastham									
1967 (29 days)	0.173	3.268	325.7°	1.016	7.9°	0.269	223.6°	8.23	67.8°

2.1 Tidal currents

Prandle *et al.* (1990) described earlier attempts at monitoring currents in this estuary using electromagnetic current meters. In a subsequent exercise (Lane *et al.*, 1997), acoustic Doppler current profiler (ADCP),

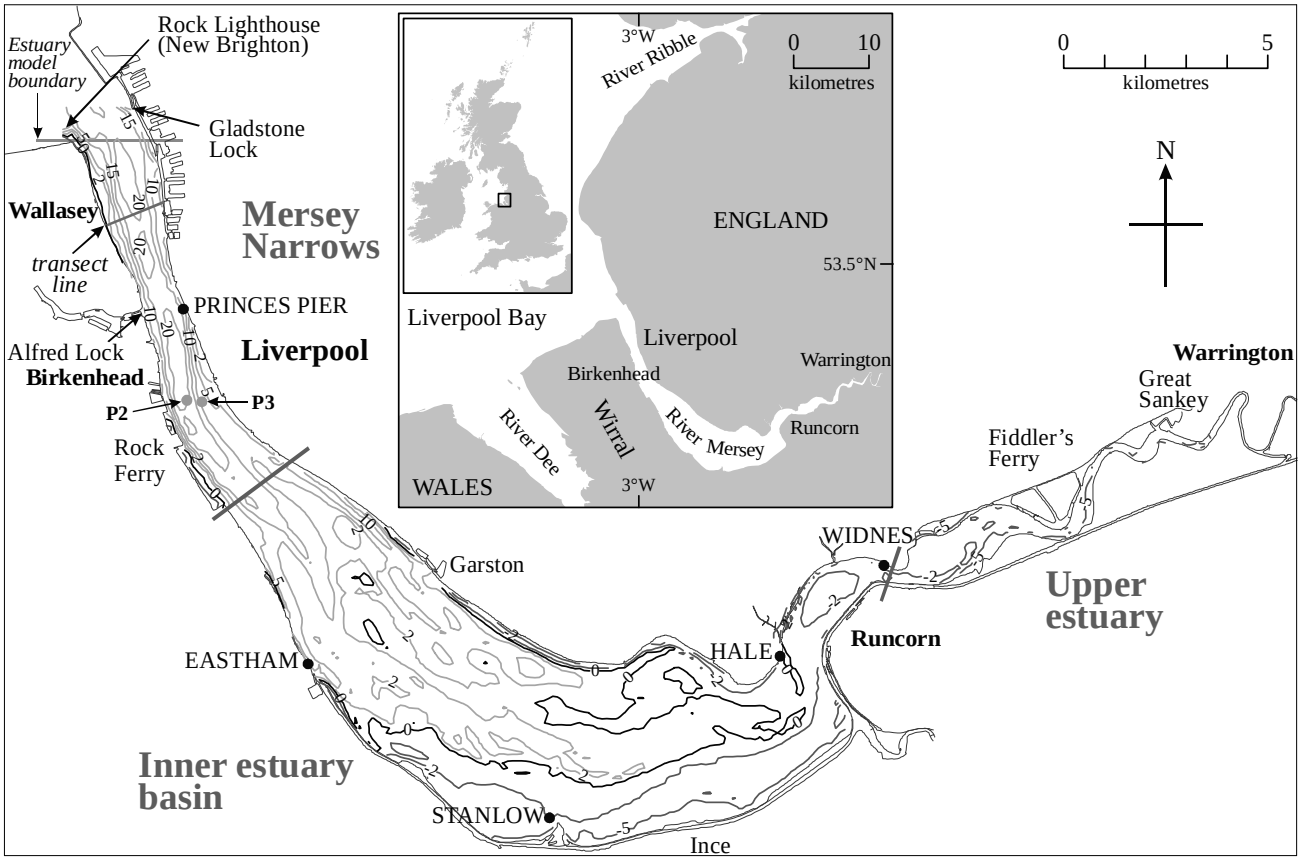

Figure 1: Liverpool Bay and the Mersey Estuary Location Map. This Shows the 1992 transect line, positions P2, P3, and tide gauges (1980 measurement sites) Marked with dots Depths (1997 bathymetry) are in metres below Ordnance Datum Newlyn (ODN). Chart datum is approximately the lowest astronomical tide level, and is 4.93 m below ODN.

electromagnetic and mechanical current meters were deployed across the Narrows at the section shown in Figure 1. Additional ADCP transects across the Narrows were made continuously over a 15-day spring-neap cycle. These measurements show that the M_2 constituent predominates; it is almost rectilinear with maximum amplitude of 1.5 m s^{-1}. The N_2 constituent has approximately half the amplitude of the S_2 constituent which, in turn, is about one-third of the magnitude of the M_2 amplitude. A simple theoretical model (Prandle, 1982) reproduces the vertical and transverse variability in the tidal current distribution– essentially a localised response to depth variations.

2.2 Suspended Sediments and Net Deposition

Figure 2 shows observed suspended sediment time series from locations in the Narrows recorded in 1986 and 1992; Table 2 summarises these results. The 1986 observations included five simultaneous moorings across the Narrows, providing estimates of net spring and neap tidal fluxes of sediments.

2.3 Past Studies

Price and Kendrick (1963) used physical scale models of Liverpool Bay and the Mersey Estuary to investigate causes of bathymetric change. The model used a grain size of 180 mm. They noted the near-bed movement of sand upstream in the Mersey by a landward current drift associated with saline intrusion–shown to extend 40 km. Without saline intrusion, the near-bed drift of sand was seawards. However, the main influence was attributed to the impact of marine sediment from a distance "beyond any possible direct influence of changes within the Mersey".

Table 2
Comparison of Lagrangian Model Results with Observations: Values in the Narrows.

Sediment settling velocity, w_s (m s^{-1})	*Susp. sediment conc. (mg l^{-1}) at position (2)* mean	max	min	*Net sediment deposited (10^3 t a^{-1})*	*Net tidal flux (10^3 m^3 s^{-1})* spring	neap	
0.005	*25*	*67*	*0*	*1800*	*46.5*	*2.3*	*Lagrangian model*
0.0005	*213*	*442*	*0*	*4900*	*306.0*	*8.8*	*Lagrangian model*
Observed in							
1986	300	1100	0		200.0[b]	60.0[b]	Observed (surface)
	500	1500	0				Observed (mid-depth)
1992 (1)	53	115*	0				
(2)	250	1500*	0				
				2300[a, c]			Bathymetric records

Position on line A-B of Figure 1:
(1) 280 m from Wirral, (2) 290 m from Liverpool shore.
[a] Lane (2004), [b] Prandle *et al.* (1990), [c] Thomas *et al.* (2002)
* 90% of sediments have concentrations less than this value

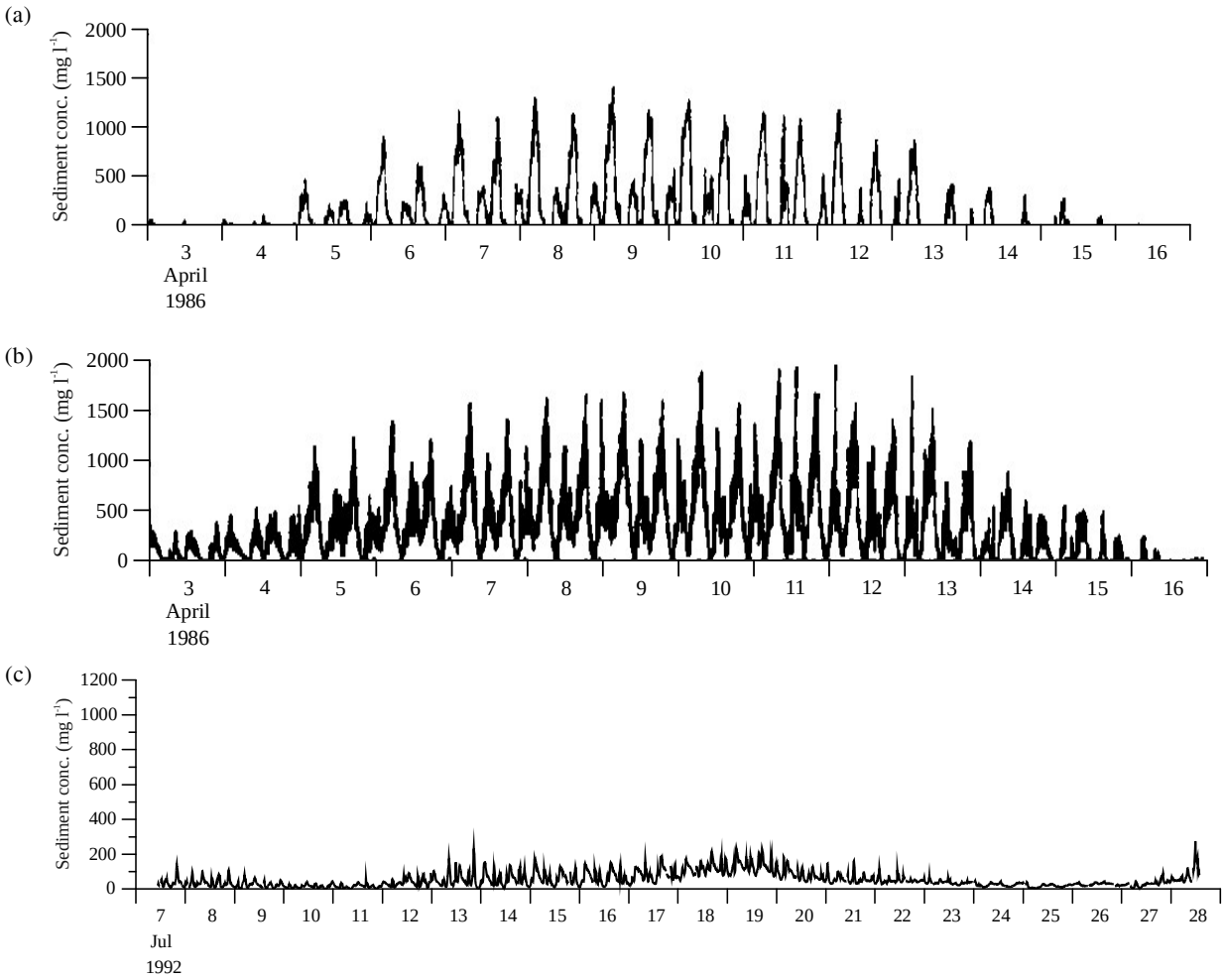

Figure 2 (a–c): Observed Sediment Concentrations in the Narrows.
(a) Surface, (b) mid depth 1986, (c) near-bed 280 m from Wirral shore 1992.

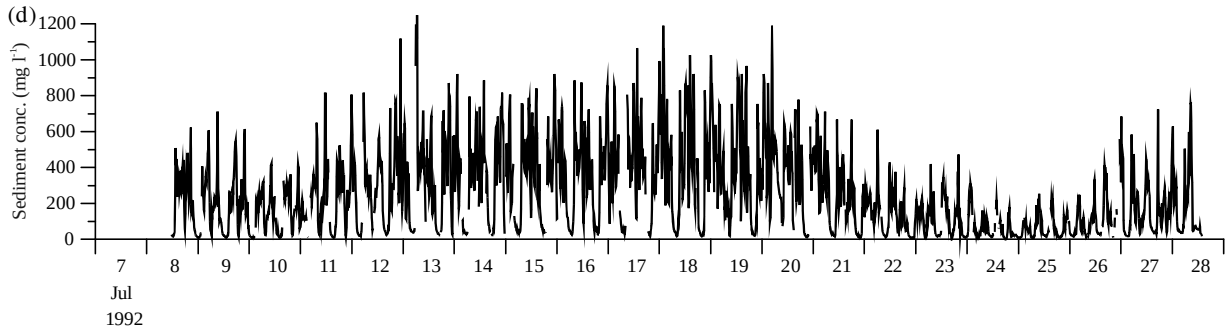

Figure 2: Observed Sediment Concentrations in the Narrows: (a) Surface, (b) Mid depth 1986, (c) near-bed 280 m from Wirral shore and (d) near-bed 290 m from the Liverpool shore 1992.

Observational surveys indicated tidal fluxes of sediment movements ranging from 3000 t (tonnes) for a tidal amplitude of 2.6 m, to 150000 t for a tidal amplitude of 4.4 m. It was noted that at their 'position 2' (P2 in Figure 1) in the Narrows, all material was finer than 76 μm (i.e., silt) whereas at 'position 3' (P3), a considerable quantity of sand was also present. Records of dredging spoils between 1955 and 1969 showed approximately equal amounts of sand and silt.

Agar and McDowell (1971) described the development of the Mersey approach channel between 1891 and 1970. They showed a progressive decrease in the volume of the inner Mersey from 750 million cubic metres (Mm^3) in 1861 to 680 Mm^3 despite dredging since 1901 at a rate of approximately 4.2 Mm^3 per year. In combination, these indicate net accretion of close to 5 Mm^3 per year.

Prandle *et al.* (1990) analysed four sets of observations of SPM indicating tidally averaged cross-sectional mean concentrations varying as a function of tidal amplitudes, ζ, as follows: 32 mg l^{-1} for ζ = 2.6 m, 100 mg l^{-1} for ζ = 3.1 m, 200 mg l^{-1} for ζ = 3.6 m and 213 mg l^{-1} for ζ = 4.0 m. These values correspond to a tidal flux (on ebb or flood) of 40000 t on a mean tide, reducing to as little as 2500 t at neap and increasing by up to 200000 t on springs–in reasonable agreement with earlier estimates of Price and Kendrick (1963).

Hutchinson and Prandle (1994) estimated net accretion rates in the adjacent and similarly sized Dee Estuary of 0.3 Mt a^{-1} between 1970 and 1990 and 0.6 Mt a^{-1} between 1950 and 1970.

Hill *et al.* (2003) derived settling velocities, w_s, of 0.0035 m s^{-1} for spring tidal conditions and 0.008 m s^{-1} for neaps. Noting that particle diameter d (μm) ≈ H" 1000 $w_s^{½}$ (m s^{-1}), these correspond to d = 59 and 89 μm, respectively.

3. ANALYSES OF OBSERVATIONAL DATA

3.1 Water Levels

Tidal constituent data from 1918 to 1993 were available from tide gauges in the River Mersey from the mouth upstream to Eastham. Data cover varying time spans although they are usually for at least one year. Lane (2004) shows a detailed analysis of the mean Z_0, semi-diurnal M_2, S_2 and quarter-diurnal M_4 constituents.

The values of the Z_0 tidal constituent at Gladstone Lock, Alfred Lock and Princes Pier (Table 1) show increasing mean sea level, while the amplitudes and phases of the semi-diurnal constituents are relatively stable.

Princes Pier has the longest record, and the largest difference encountered here is an increase of about 0.1 m in the M_2 amplitude, with most variability occurring before 1930. Before 1930, phases vary by less than 1°, while since 1960 a slight phase lead of 2° developed.

At Gladstone Lock and Alfred Lock, phases vary by less than 0.5°. M_2 amplitudes are fairly consistent over time (1964–1994), although they increase by about 0.05 m in the 5 km from Gladstone Lock to Princes Pier.

Alfred Lock on the opposite shore shows an unexpected increase in amplitude of 0.05 m after 1964. Woodworth *et al.* (1999) note that the mean sea level (at Gladstone Lock) rose by some 170 mm over the period 1858–1998.

3.2 Bathymetry

Data are available from surveys carried out by the Mersey Docks and Harbour Company in 1906, 1936, 1956, 1977 and 1997. Water volumes in the estuary below highest astronomical tide level were computed from these (Figure 3). The overall pattern is for the estuary volume to decrease by about 60 Mm^3 or 8% between 1906 and 1977, despite sea level rise averaging 1.23 mm per year during the past century noted by Woodworth *et al.* (1999). After this period, there is a small increase of 10 Mm^3. An Empirical Orthogonal Function (EOF) analysis of the five bathymetric data sets confirmed a gradual decrease totalling 3.9% of the initial value between 1936 to 1977 (compared with 5% as in Figure 3), followed by a slight increase of 0.4% after 1977.

Differences in volume within the Narrows are of the order of a few percent from one data set to the next. The largest changes appear in the inter-tidal regions of the inner estuary basin, particularly from Hale and Stanlow to Runcorn where the low water channel positions change readily, and differences between successive surveys have exceeded 10%.

Tidal propagation responds immediately and directly to changes in bathymetry and, to a lesser degree, to variations in bed roughness determined by surficial sediments. Sediment transport patterns modulate this response providing a longer term balance. Asymmetries in the ebb and flow sediment fluxes adjust until an equilibrium state is restored (Friedrichs and Aubrey, 1988; Dronkers, 1998).

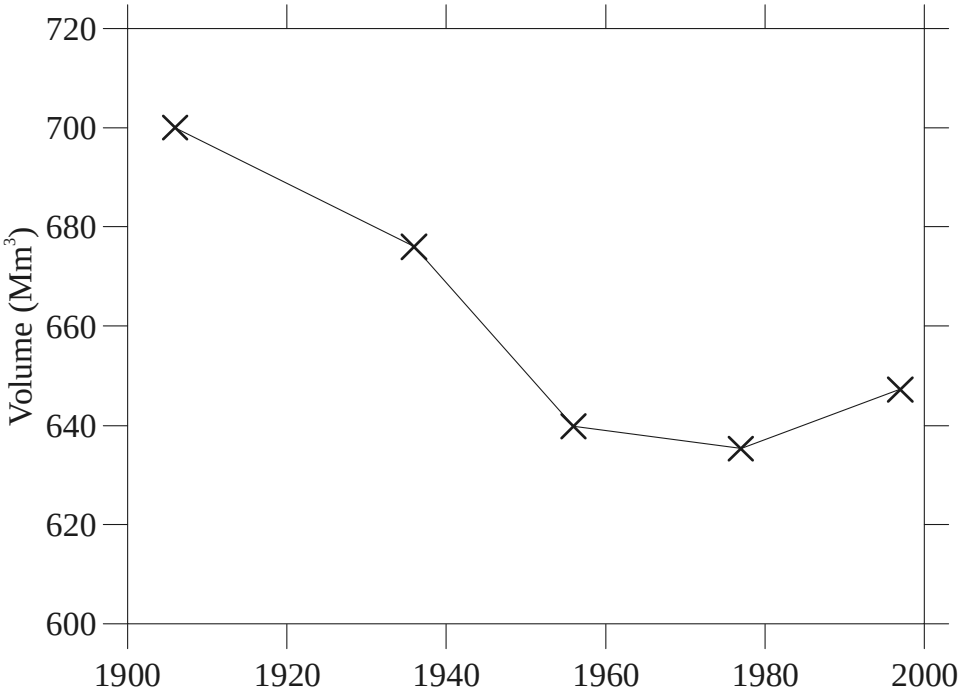

Figure 3: Total Water Volumes in the Mersey Estuary. Volume below the highest astronomical tide level at Gladstone Lock (5.1m above Ordnance Datum Newlyn) in millions of cubic metres, calculated from the bathymetry data sets 1906–1997.

The above analyses are in broad agreement with that of Thomas *et al.* (2002). They show the likely influence of training wall construction and dredging of approach channels in the earlier decrease in volume. A subsequent adjustment towards a stable state is attributed to a reduction in the supply of marine sediments.

4. THEORETICAL IMPACTS FROM GLOBAL CLIMATE CHANGE

4.1 Impacts on Tide and Surge Heights

Indications of likely changes to the estuarine response of tides and surges are investigated using the analytical expressions derived by Prandle and Rahman (1980) subsequently referred to as 'PR'.

We adopt three characteristic shapes namely: BAY, LINEAR and FUNNEL described by axial, x, variations in breadth and depth increasing in proportion to $x^{½}$, x and $x^{3/2}$ respectively. These shapes correspond to values of the funnelling parameter, ν (in PR) of 1, 2 and 5, i.e., almost the complete range of estuaries encountered.

Figure 3(b) of PR shows that over this range ($1 < \nu < 5$), amplification of tides (and surges) between the first 'node' and the head of the estuary can be up to a factor of 2.5. Concern focuses on conditions in estuaries where the bathymetric dimensions (length, depth and shape) result in the estuarine mouth coinciding with this node, for the excitation 'period', P, with consequent resonant amplification. This occurs when

$$y = 0.75\nu + 1.25 \tag{1}$$

with

$$y = \frac{4\pi L}{P(2-m)(gD)^{½}}, \tag{2}$$

where L and D are the estuarine length and depth (at the mouth), and m is the power of axial depth variation (0.5, 1 or 1.5 noted above).

Figure 4 indicates the corresponding resonant periods for a range of both L and D. Results for $m = 1$ are within 10% of those for $m = 0.5$ and $m = 1.5$, hence only those for $m = 1$ are shown.

By utilising the formula the formula:

$$L = \frac{120D^{5/4}}{(f\zeta)^{½}} \tag{3}$$

derived by Prandle (2003), with the bed friction coefficient, $f = 0.0025$ and ζ tidal elevation amplitude, we derive the following expressions for resonant values of L and D:

$$L \sim 2500P^{5/3}\zeta^{1/3} \tag{4}$$

and

$$D \sim P^{4/3}\zeta^{2/3}$$

with P in hours and ζ, D and L in metres.

These equations indicate that resonance at semi-diurnal frequencies will only occur for $D > 25$ m and $L > 150$ km. The tidal reach of the Thames is approximately 95 km and the Humber 60 km. Hence, we only anticipate resonance for the semi-diurnal frequency in systems such as the Bristol Channel where the estuarine 'resonance' extends to the adjacent shelf sea. Thus, we do not expect dramatic changes in tide and surge responses in UK estuaries for anticipated changes in sea level of up to 1 m. Likewise increases in flood levels due to rises in mean sea level are likely to be of the same order as the respective increases in adjacent open-sea conditions.

Some exception to the above is possible for surge response to secondary depressions prevalent along the West Coast which can have effective periodicities of significantly less than 12 hours and hence may have resonant responses as indicated in Equation (4).

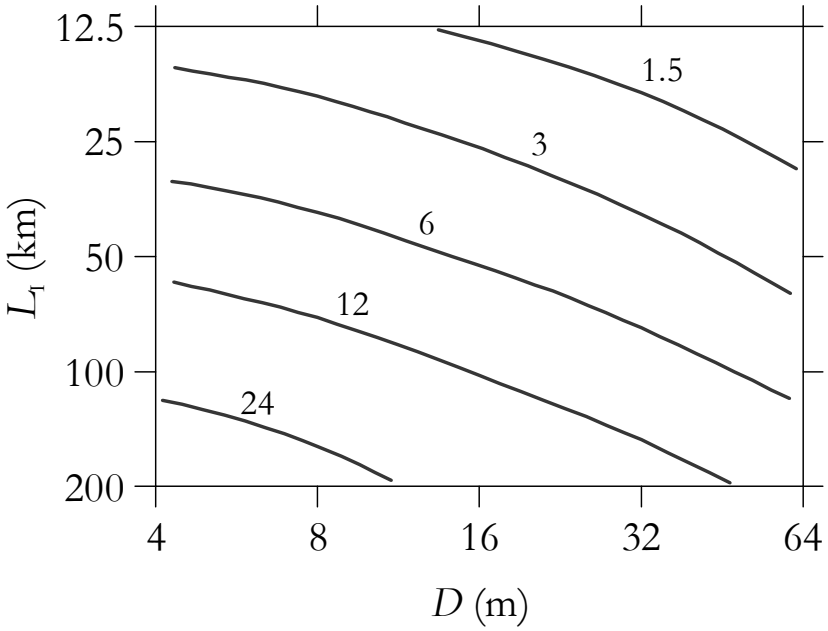

Figure 4. Resonant Periods of an Estuary. The period (in hours) is a function of estuarine length and depth (at the mount)

4.2 Intervention

Prandle (1989) examined the change in tidal response in estuaries due to variations in mean sea level where the locations of the coastal boundaries remain fixed (i.e., construction of flood protection walls). The results show the largest impacts will be in flat, shallow estuaries.

4.3 Impacts on Morphology of Changes in Mean Sea Level and River Flows

Prandle (2004a) developed new theories for estuarine bathymetry applicable to the tidally dominated coasts encountered around the UK. UK estuaries include large inter-tidal zones, with breadths at high tide typically three or more times low tide values. Hence, the theoretical developments assumed triangular cross sections with side-slope $a = 2D / B$. These theories provide explicit formulations for estuarine length (Equation 3) and:

(i) depth at the mouth, D, as a function of river flow, Q

$$D = 12.8(Qa)^{0.4} \tag{5}$$

where a is the side-slope gradient.

(ii) salinity intrusion length L_I

$$L_I = \frac{0.005D^2}{f\,U\,U_0} \tag{6}$$

where U is tidal current amplitude and U_0 the current associated with river flow.

(iii) a bounded zone of likely estuarine morphologies defined by:

$$E_X / L < 1$$
$$L_1 / L < 1 \tag{7}$$
$$\text{and } D / U^3 < 50 \text{ (m}^{-2}\text{ s}^3\text{)}$$

where E_X is the tidal excursion length and D / U^3 the Simpson and Hunter (1974) criterion for 'mixed' waters.

An extensive database for UK estuaries, 'FutureCoast' (Burgess *et al.*, 2002), was used to establish the validity of the above theories (Prandle *et al.*, 2006). Figure 5 shows how the conditions (7) bound the morphology of almost all of the estuaries from this data set. Having established the validity of the above morphological expressions, Figure 5 provides immediate estimates of the impact of changes in mean sea level or river flow on any specific estuary.

Estimates of 'precautionary' changes in sea level and river flows by 2100 (Defra/Environment Agency Technical Summaries, 2003 and 2004) amount to an increase of 50 cm and both increases and decreases of up to 25% respectively.

Inserting these changes in river flow, Q, in (5) and the resulting changes in depth, D, into (3) we can estimate the changes in length, L. Likewise the changes in breadth, B, associated with the changes in D can be estimated by assuming the side-slope gradients, a, are unchanged. Table 3 shows these resultant changes. The changes, δD, in D correspond to $\delta Q^{0.4}$, changes in L to $(\delta Q^{0.4})^{1.25}$ and to B to $2\delta D/a$. The results show that, on average, the 'dynamical' adjustment to a 25% change in river flows may change depths as much as the projected sea level rise–with this effect reduced in smaller estuaries and significantly increased in larger ones. The resulting changes in estuarine lengths and breadths follow similar patterns with the biggest 'dynamical' change occurring in the largest estuaries where they are significantly greater than those due to sea level rise. Overall we anticipate changes in: estuarine lengths of the order of 0.5 to 5 km and breadths of the order 50 to 250 m due to the 25% change in river flow. Corresponding changes due a sea level rise of the order 50 cm are increases in both lengths of order 1 to 2.5 km and breadths of 70 to 100 m.

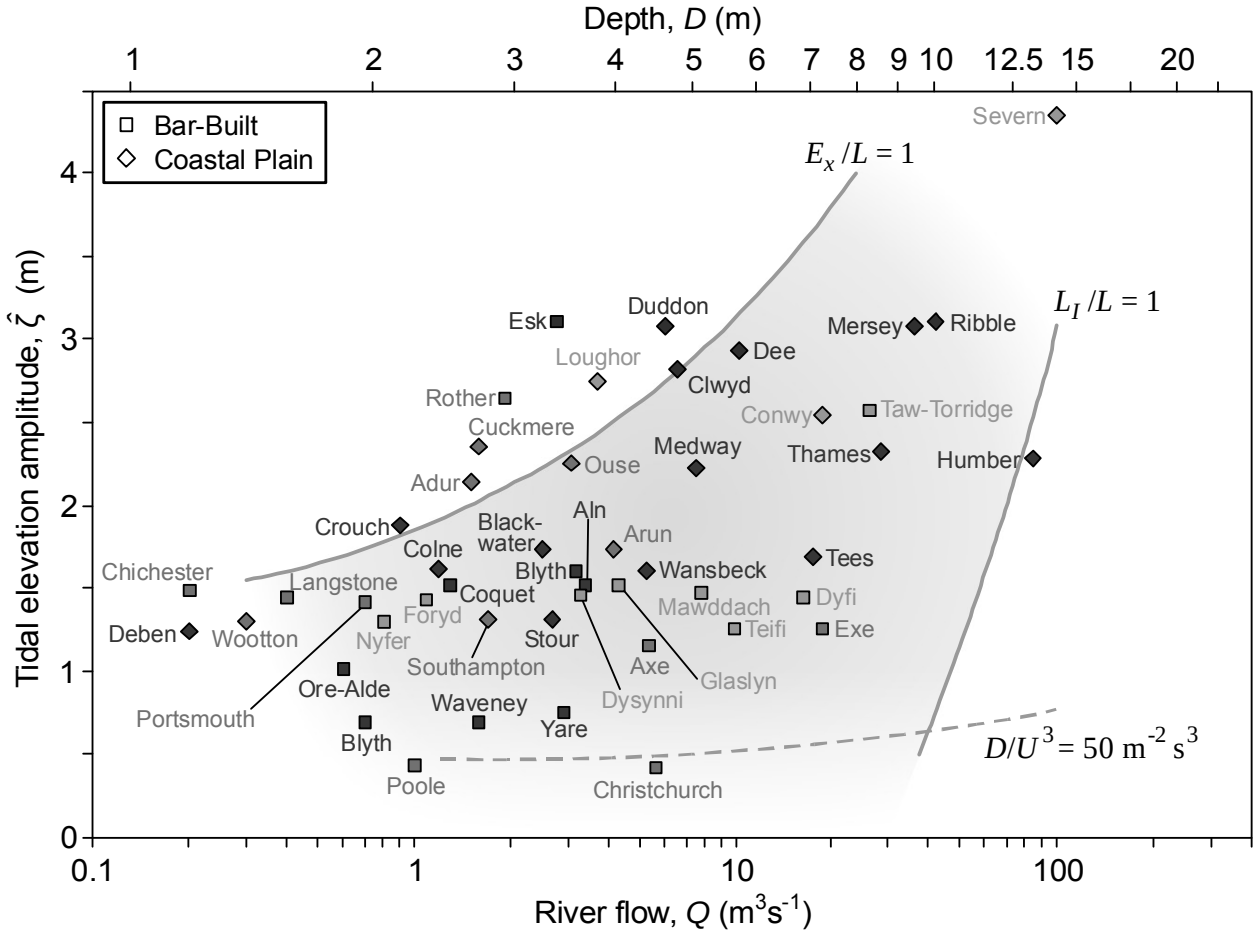

Figure 5. Zone of Morphological Existence (Equation 7).

Table 3
Changes in Estuary Dimensions with River Flow and Mean Sea Level (msl).
Depth D, length L, breadth B; river flow Q

Estuary type		$D(m)$	δD_Q +/–	$L(km)$	δL_Q +/–	δL_{msl} +	B (m)	δB_Q +/–	δB_{msl} +	
All	min.	2.5	0.25	5	0.62	1.28	130	38	}	
	mean	6.5	0.65	20	2.50	1.94	970	100	}	77
All	max.	17.3	1.73	41	5.12	1.49	3800	266	}	
Coastal Plain		8.1	0.81	33	4.12	2.57	1500	147	91	
Bar-Built		3.6	0.36	9	1.12	1.59	510	51	71	

4.4 Change in Sediment Supply

The dynamical theories do not consider the sediment regimes in estuaries. Changes in the nature and supply of marine sediments (supply of fluvial sediments to most UK estuaries is negligible in terms of its influence on morphology) can lead to abrupt changes in estuarine morphology. This supply can directly determine the nature of the surficial sediments and thereby bed roughness. Peculiarly, the derived relationship (Equation 5) between depth at the mouth and river flow is independent of both tidal amplitude and bed roughness. However, from (Equation 3), the associated estuarine length will shorten as sediments become coarser.

Prandle (2004b) explored the conditions necessary to maintain quasi-equilibrium between tidal dynamics and zero net import/export of sediments. This resulted in a paradigm shift suggesting that the prevailing sediment regime is a consequence of rather than the determinant for estuarine morphology. Moreover a stabilising feedback was shown whereby both the balance between import/export of sediments and the whole-estuary tidal energetics are directly related to the phase difference between elevations and currents.

5. NUMERICAL MODELLING

Morphological adjustments can occur over time scales from decades to millennia (Prandle, 2003b). Here we assess the capabilities and limitations of a 3-D Eulerian Hydrodynamic model coupled with a Lagrangian sediment module (Lane and Prandle, 2006) to quantify impacts on estuarine sediment regimes and indicate the rate and nature of bathymetric evolution. Particular emphasis is on quantifying the variations in sediment concentrations and fluxes in sensitivity tests of: bed roughness, eddy viscosity, sediment supply (particle sizes 10 to 100 μm), salinity intrusion and 2-D versus 3-D formulations of the hydrodynamic model. The model was not intended to reproduce bed-load transport associated with coarser sediments.

Recognising the limited capabilities to monitor the often extremely heterogeneous suspended particulate matter, a wide range of observational data was used for assessing model performance. These include: suspended concentrations (axial profiles of mean and '90th percentile'), tidal and residual fluxes at cross-sections, estuary-wide net suspension and deposition on spring and neap tides, surficial sediment distributions and sequences of bathymetric evolution.

5.1 Model Description

A 3-D Eulerian (fixed-grid) hydrodynamic model provides velocities, elevations, and diffusivity coefficients for a Lagrangian 'random-walk' particle model in which up to a million particles represent the sediment movements.

An existing 3-D finite-difference model based on POLCOMS (the Proudman Oceanographic Laboratory Coastal-Ocean Modelling System) was used. It includes a wetting-drying scheme to account for the extensive inter-tidal areas. Forcing involved specifying tidal elevation constituents at the seaward limit in the Mersey

Narrows, and river flow at the head. The model uses a 120-metre rectangular grid horizontally and a 10-level sigma-coordinate scheme in the vertical. The detailed bathymetry data sets of the Mersey, described in Section 2, were used.

Calibration of the model (Lane, 2004) involved simulating effects of 'perturbations' (based on varying the mean sea level, bed friction coefficient, vertical eddy viscosity and the river flow) and finding the optimum combination to minimise differences from observed constituents for elevations. The model indicated that the estuary (particularly in the inner estuary basin) is most sensitive to changes in bathymetries and bed friction coefficients. River flow only has an appreciable effect for discharges significantly higher than those usually encountered.

5.2 Lagrangian, Random-walk Particle Module for Non-cohesive Sediment

Random-walk particle movements are utilised to replicate solutions of the Eulerian advection-diffusion equation (Fischer *et al.*, 1979),

$$\frac{\partial C}{\partial t} + u\frac{\partial C}{\partial x} + v\frac{\partial C}{\partial y} - w_s\frac{\partial C}{\partial z} = \frac{\partial}{\partial z}(K_z\frac{\partial C}{\partial z}) + \text{source} \tag{8}$$

change in concentration advection setting diffusion

where C is the suspended sediment concentration, u and v are orthogonal velocity components, w_s is the fall velocity, and K_z is the vertical eddy diffusivity coefficient.

The Lagrangian module involves calculations, for successive time steps, of the height above the bed, z and horizontal location of each particle following:

(i) a vertical advective movement $-w_s\Delta t$ (downwards)

(ii) a diffusive displacement l (up or down),

(iii) horizontal advection.

Additional new particles are released into suspension by accumulation of the erosion potential; likewise particles may be 'lost' by settlement following the advective movement in (i).

Erosion

A simple algorithm for the erosion source was adopted

$$\text{ER} = \gamma f \rho U^p \quad (\text{kg m}^{-2}\,\text{s}^{-1}) \tag{9}$$

where f is the bed friction coefficient and ρ is water density. The power p, to which the tidal velocity is raised, is selected as 2 here–setting the erosion rate directly proportional to the magnitude of frictional stress at the bed. Having specified p, all subsequent calculations of concentration, flux and sedimentation rates are linearly proportional to the coefficient γ. A value of $\gamma = 0.0001$ m^{-1} s was found to produce suspended sediment concentrations comparable with those in Figure 2. The corresponding values of tidal and residual cross-sectional fluxes were also in reasonable agreement with observed values shown in Table 2; hence this value for γ was used throughout.

Settlement

Deposition occurs when the height of the particle above the bed calculated in a discrete advective settlement step $-w_s\Delta t$ is less than zero.

Diffusion

Particles are displaced upwards or downwards randomly by a length $l = \sqrt{(2 K_z \Delta t)}$ (Fischer *et al.*, 1979). K_z is approximated by $f\hat{U}D$ (Prandle, 1982). Contacts with the surface and bed during this diffusion step are reflected elastically.

Operation

Starting with no sediment in the estuary, all particles are introduced at the seaward boundary of the model using the erosion formula (Equation 9). An unlimited supply is assumed together with zero axial concentration gradient ($dC/dx = 0$) for inflow conditions. To reflect the effect of changing distributions of surficial sediments on the bed friction coefficient, this was specified as $0.0158\, w_s^{1/4}$.

Sensitivity Tests

Full details of the sensitivity tests are shown by Lane and Prandle (2006), these are summarised in Table 4.

Figure 6 shows time series over two spring-neap cycles (commencing from the initial introduction of sediments) of the cross-sectional mean suspended sediment concentration at successive locations landwards from the mouth. The examples chosen are for sediment fall velocities, w_s of 0.005 m s^{-1} (coarse sediment $d = 70$ μm, black lines) and 0.0005 m s^{-1} (finer sediment, $d = 22$ μm, grey lines) respectively.

For $w_s = 0.0005$ m s^{-1} (grey lines), the suspended sediment time series change from predominantly semi-diurnal (linked to advection) at the mouth to quarter-diurnal (linked to localised resuspension) further upstream. Even close to the mouth, a significant quarter-diurnal component is generated at spring tides. Close to the mouth, peak concentrations occur some three tidal cycles after maximum spring tides and at up to seven cycles later further upstream.

For the coarser sediment, $w_s = 0.005$ m s^{-1} (black lines), Figure 6 shows much reduced concentrations largely confined to the seaward region, although the slower 'adjustment' rate suggests that a longer simulation is required to introduce the coarser sediments further upstream. The time series is predominantly quarter-diurnal and peak concentrations coincide with peak tides; the sediments have a much shorter half-life in suspension Prandle (1997).

Figure 7(a) shows corresponding time-series of cumulative inflow and outflow of sediments across the mouth of the estuary model. Differences between inflow and outflow, in Figure 7(b), indicate net suspension (high frequency) and net deposition (low-frequency). For $w_s = 0.0005$ m s^{-1}, the mean tidal exchange of sediments is around 110000 t per tide, of which approximately 6% is retained amounting to 7000 t per tide. For $w_s = 0.005$ m s^{-1}, the mean exchange is 22000 tonnes of which approximately 12% is retained or about 3000 t per tide.

5.3 Sensitivity to Sediment Size

For a more extensive quantitative evaluation of the model, single neap-spring tidal cycle simulations were used. Results are summarised in Table 4(a) for particle diameters d from 10 to 100 μm.

The model reveals that mean suspended sediment concentrations vary approximately with d^{-2}. Equation (43) of Prandle (2004a) indicates variability ranging from d^0 to d^{-4} for finer to coarser sediments. The extent of landward intrusion increases progressively for finer sediments. A minimum capture rate of 2.8% occurs for $d = 30$ μm with a corresponding deposition rate of 1 Mt per year. While capture rates increase progressively with increasing sediment size (above $d = 30$ μm), corresponding decreases in concentration yield a maximum deposition at 50 μm of 2 Mt per year. This maximum is close to the preponderance of sediments with $w_s = 0.003$ m s^{-1} ($d = 54$ μm) found by Hill *et al.* (2003). Prandle (2004b) calculated the size of suspended sediments corresponding to 'equilibrium' conditions of zero net deposition or erosion to be in the range 20 to 50 μm. Net sedimentation remains surprisingly constant, between 1 and 2 Mt per year, throughout the range of $d = 30$ to 100 ìm. This sedimentation rate is in close agreement with observational evidence (Section 3).

5.4 Sensitivity to Model Parameters

The model's responses to the following parameters were quantified: vertical structure of currents, eddy diffusivity and salinity, as well as the bed friction coefficient and sediment supply.

Table 4
Sensitivity of Modelled Sediments

(a) particle diameters d = 10 to 100 μm for w_s(m s^{-1}) ≈ 10^{-6} d(μm)^2

d(μm)	Mean suspended sediment concentrations (mg l^{-1}) at 2 km intervals upstream from the mouth																
10	1645	1465	1423	1183	1118	1049	875	669	562	418	252	177	173	119	106	81	92
20	176	157	151	128	120	108	93	75	60	43	27	17	15	8	7	5	5
30	68	56	47	34	27	20	14	8	4	2	1	-	-	-	-	-	-
40	51	41	33	22	17	11	6	3	1	1	-	-	-	-	-	-	-
50	41	33	27	19	14	8	4	2	1	-	-	-	-	-	-	-	-
60	32	26	20	14	10	5	2	-	-	-	-	-	-	-	-	-	-
70	23	19	15	10	7	3	-	-	-	-	-	-	-	-	-	-	-
80	18	14	11	7	5	2	-	-	-	-	-	-	-	-	-	-	-
90	13	10	8	5	3	1	-	-	-	-	-	-	-	-	-	-	-
100	10	8	6	3	2	-	-	-	-	-	-	-	-	-	-	-	-

d(μm)	90th percentile suspended sediment concentrations (mg l^{-1}) at 2 km intervals upstream from the mouth																
10	4186	3896	3804	3366	3274	3167	2471	1525	1052	714	560	470	500	348	309	217	162
20	369	344	325	297	258	240	218	183	140	84	52	37	36	20	19	20	12
30	169	148	133	101	89	67	47	29	12	6	3	2	2	-	-	-	-
40	140	118	103	75	64	45	26	12	5	3	2	1	1	-	-	-	-
50	108	95	83	62	53	35	16	7	4	3	2	1	1	-	-	-	-
60	83	72	65	47	39	22	8	3	1	-	-	-	-	-	-	-	-
70	63	56	50	38	29	16	5	1	-	-	-	-	-	-	-	-	-
80	50	45	40	30	22	11	2	-	-	-	-	-	-	-	-	-	-
90	39	35	29	22	16	7	-	-	-	-	-	-	-	-	-	-	-
100	31	29	25	17	12	4	-	-	-	-	-	-	-	-	-	-	-

	Suspended		*Deposited*		*Exchange*		*Deposited*	*% deposit*	*Average*
d(μm)	*neap*	*spring*	*neap*	*spring*	*neap*	*spring*	*per year*	*/exchange*	*suspended*
10	156.21	1531.12	28.40	420.84	57.53	2508.81	66400	10.5	640.06
20	2.15	206.55	–0.99	61.07	9.80	490.07	5000	5.9	75.75
30	3.97	34.77	–0.67	4.93	5.86	106.96	1000	2.8	15.03
40	2.31	22.62	–0.54	5.06	5.51	87.48	1200	4.4	9.46
50	1.77	18.07	–0.05	6.12	4.14	71.20	1400	6.2	7.47
60	1.13	12.97	–0.04	7.15	3.21	58.85	2000	10.5	5.19
70	0.79	9.28	0.56	6.49	2.93	43.83	1800	12.3	3.69
80	0.58	7.36	0.23	7.64	2.02	36.91	1700	14.0	2.87
90	0.41	5.48	0.14	7.54	1.70	30.55	1600	16.9	2.11
100	0.26	4.48	0.10	5.62	1.15	25.09	1400	18.6	1.64

Units: 10^3 tonnes

(b) Diameter 22 μm, w_s = 0.0005 m s^{-1}

Run	*Mean suspended sediment concentrations (mg l^{-1}) at 2 km intervals upstream from the mouth*																
1)	127	109	98	77	67	58	47	34	25	16	10	6	4	2	2	1	1
2)	333	304	301	263	253	234	205	171	141	106	71	50	49	35	29	23	25
3)	132	117	112	95	89	79	69	58	48	36	26	17	17	8	7	5	5
4)	127	112	104	84	76	69	56	43	32	21	12	7	5	2	2	1	1
5)	48	42	40	33	31	28	22	17	14	10	7	5	4	1	1	1	1
6)	196	171	155	127	116	105	86	60	42	24	12	7	5	2	1	1	1
7)	73	65	60	49	44	38	30	23	16	10	5	2	2	-	1	-	-
8)	**125**	**109**	**102**	**84**	**76**	**67**	**55**	**44**	**34**	**23**	**14**	**8**	**7**	**3**	**2**	**2**	**1**

Table 4. (continued)

Run	*90th percentile suspended sediment concentrations (mg l^{-1}) at 2 km intervals upstream from the mouth*																
1)	290	250	229	182	166	144	118	86	63	40	24	16	16	10	9	7	9
2)	807	783	799	742	703	615	534	420	336	206	147	111	98	72	63	55	45
3)	279	259	257	218	208	186	171	148	114	81	63	48	52	31	24	22	18
4)	277	249	237	188	177	165	141	115	77	44	24	17	15	8	6	4	3
5)	90	84	82	70	67	62	53	44	37	28	18	16	16	8	6	7	5
6)	388	347	328	265	254	240	210	151	90	55	33	22	17	8	7	5	1
7)	149	137	133	107	99	93	81	59	36	18	11	8	7	4	4	1	1
8)	**278**	**250**	**245**	**199**	**183**	**163**	**148**	**121**	**82**	**46**	**29**	**21**	**19**	**10**	**7**	**8**	**5**

Run	*Suspended*		*Deposited*		*Exchange*		*Deposited per year*	*% deposit /exchange*	*Average suspended*
	neap	*spring*	*neap*	*spring*	*neap*	*spring*			
1)	8.58	70.21	–0.88	10.73	9.14	182.69	2200	3.8	31.03
2)	21.91	476.73	–1.20	118.22	11.49	1020.43	9300	5.9	167.55
3)	8.60	124.63	–1.17	30.70	8.41	289.48	3200	5.1	47.21
4)	7.78	121.18	–0.99	26.61	7.72	285.81	2700	4.3	45.21
5)	4.08	23.55	–0.58	2.83	4.44	60.80	800	3.5	11.84
6)	19.11	134.84	–1.51	23.94	17.92	310.08	3000	3.6	62.73
7)	6.62	61.39	–0.48	6.31	5.28	134.45	800	2.6	26.10
8)	**8.32**	**116.75**	**–1.59**	**24.30**	**6.71**	**271.36**	**2500**	**4.2**	**44.54**

Units: 10^3 tonnes

(1) No vertical shear in currents, i.e., a 2-D hydrodynamic model.

(2) Depth-varying eddy diffusivity with depth-mean value $\bar{K}_z$ at the bed, 1.33 $\bar{K}_z$ at $z = 0.33$ and 0 at the surface, $K_z(z) = \bar{K}_z\ (-3z^2 + 2z + 1)$.

(3) A time varying value of $K_z(t)$, with a quarter-diurnal variation of amplitude 0.25 $\bar{K}_z$ producing a peak value one hour after peak currents.

(4) Mean salinity-driven residual current profile (Prandle, 1985),
$U_z = g\, S_x\, D^3 / E\,\{-0.1667\, z^3 + 0.2687\, z^2 - 0.0373z - 0.0293\}$, where the salinity gradient S_x was specified over a 40 km axial length and eddy viscosity $E = K_z$.

(5) Bed friction coefficient halved, $f = 0.5 \times 0.0158\, w_s^{1/4}$.

(6) Bed friction coefficient doubled, $f = 2.0 \times 0.0158\, w_s^{1/4}$.

(7) Erosion rate at mouth 0.5 γ, i.e., halving the rate of supply of marine sediments.

(8) BASE-LINE simulation.

Table 4(b) shows, for $w_s = 0.0005$ m s^{-1} ($d = 22$ μm), the sensitivity to:

(1) No vertical current shear, i.e., a 2-D hydrodynamic model.

(2) Depth-varying eddy diffusivity with depth-mean value $\overline{K_z}$ at the bed, 1.33 $\overline{K_z}$ at $z = 0.33$ and 0 at the surface, $K_z(z) = \overline{K_z}\ (-3z^2 + 2z + 1)$.

(3) A time varying value of $K_z(t)$, with a quarter-diurnal variation of amplitude 0.25 K_z producing a peak value one hour after peak currents.

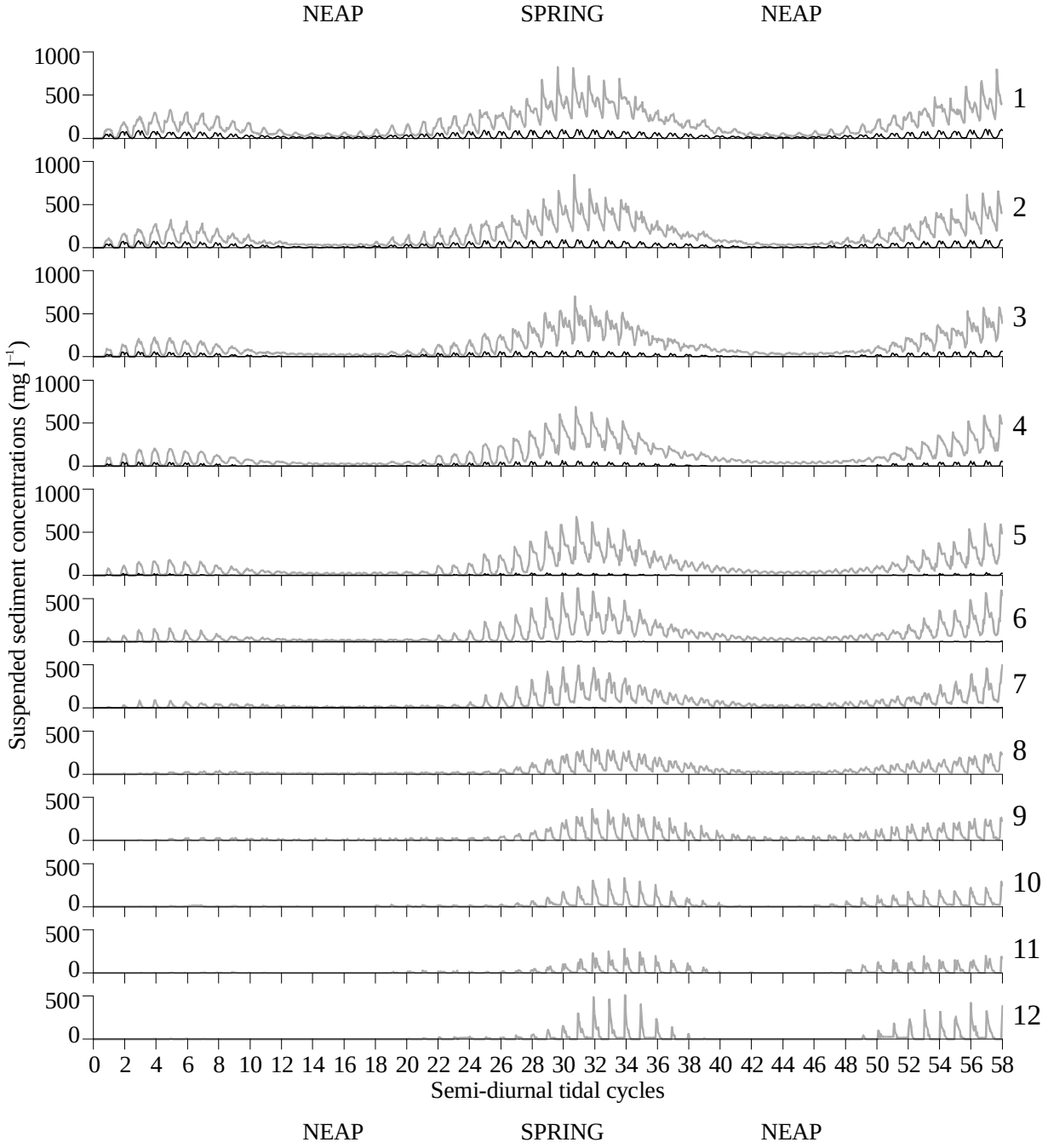

Figure 6. Suspended Sediment Concentrations at 12 positions along the Mersey. Positions are approximately km apart starting with 1 at the mouth. Grey lines–setting velocities w_s – 0.0005 ms^{-1}; black lines – w_s – 0.005 m s^{-1}.

(4) Mean salinity-driven residual current profile (Prandle, 1985),

$U_z = g\, S_x D^3 / E \{-0.1667\, z^3 + 0.2687\, z^2 - 0.0373 - 0.0293\}$, where the salinity gradient S_x was specified over a 40 km axial length and eddy viscosity $E = K_z$.

(5) Bed friction coefficient halved, $f = 0.5 \times 0.0158\, w_s^{1/4}$.

(6) Bed friction coefficient doubled, $f = 2.0 \times 0.0158\, w_s^{1/4}$.

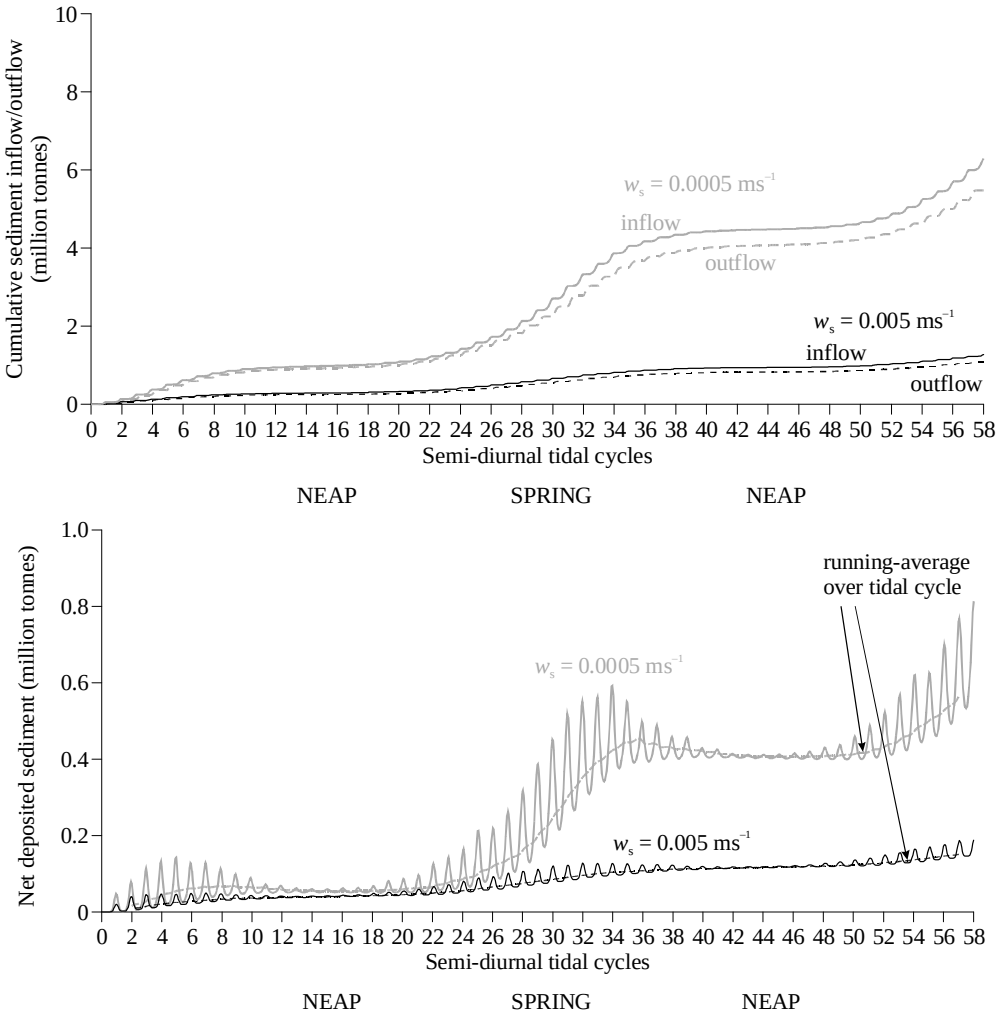

Figure 7. Sediment Transport from the Mersey Estuary Model.
(a) Comulative inflow and outflow at the mouth, (b) net suspension (high frequency) and deposition (low frequency)

(7) Erosion rate at mouth 0.5 γ, i.e., halving the rate of supply of marine sediments.

(8) BASE-LINE simulation.

While the calculated values of sediment concentration and net fluxes varied widely and irregularly for varying sediment sizes, the net deposition remained much more constant.

The acute and complex sensitivity to bed roughness and related levels of eddy diffusivity and viscosity is evident from Table 4(b). This acute sensitivity to bed roughness and sediment supply leads to concern that migration of new flora and fauna might lead to 'modal shifts' with potentially catastrophic consequences. To comprehend these sensitivities, we can approximate, from Prandle (2004b), the following dependencies on the friction factor 'f':

tidal velocity amplitude	$U \sim f^{-½}$,	
sediment concentration	$C \sim f^{½}$,	(10)
tidal sediment flux	$UC \sim f^{0}$,	
residual sediment flux	$<UC> \sim UC\,\theta \sim f^{½}$,	

where θ is the phase lag of tidal elevation relative to currents and residual sediment flux corresponds to net upstream deposition. These theoretical results are consistent with the increases in concentration and residual fluxes for larger values of *f* shown by the model for both sediment types. However, contrary to the above theory, calculated tidal sediment fluxes do show variations with *f*.

By introducing all sediments at the open boundary, the sensitivity to changes in marine supply, Run **(7)**, is immediately evident. Thus a 50% reduction in supply at the mouth reduced concentrations by nearly a half, capture rates reduced to a factor of 0.6, and deposition to one quarter. Since many estuaries will have marine supplies substantially below the maximum 'carrying capacity' assumed here, we anticipate typical capture rates and net sedimentation to be much less than those shown in Table 4. However, this sensitivity does highlight the potential for accelerated deposition rates in many estuaries if the marine supply increases (e.g., by dredging disposal or sea-bed disturbance in the offshore approaches). Using the computed patterns of bed 'sorting' (i.e., varying axial distributions of deposited sediments), each sediment size can be compared with distributions of surficial sediments to indicate the nature and quantity of the marine source.

6. SUMMARY

Historical Analyses

A century of bathymetric surveys of the Mersey indicate a net loss of estuarine volume of about 0.1%, or 1 million cubic metres, per year. Similar results are found in many of the large estuaries of NW Europe. In contrast, sea level rise of 1.2 mm a^{-1} represents only a 0.02% annual increase. This relative stability persists in a highly dynamic regime with suspended sediment concentrations exceeding 2000 mg 1^{-1} and spring tide fluxes of order 200000 t. Detailed analyses of the bathymetric sequences indicate most significant changes occur in the upper estuary and in inter-tidal zones. A long period, up to 63 years, of tidal elevation records (in the lower estuary) shows almost no changes to the predominant M_2 and S_2 constituents.

Theory

New theories provide dynamically-based algorithms for tidal bathymetry Prandle, 2003). These theories have been assessed against a database for 80 UK estuaries (Prandle *et al.*, 2006) Overall, good agreement was found between theory and observations for the sizes and shapes of estuaries classified as either 'Coastal Plain' or 'Bar Built'.

The identification of a 'zone of bathymetric existence' (Figure 5) constrained within minimum and maximum values for D, Q and ζ provides an immediate visual indication of the likely stability and sensitivity of any particular estuary.

These encouraging agreements enable these theories to be used for: (i) enhancing our understanding of existing morphologies, (ii) identifying anomalous estuaries and (iii) making future predictions regarding likely impacts from Global Climate Change and related management scenarios.

By 2100, we anticipate changes in UK estuaries due to ('precautionary') projected 25% changes in river flow of: order 0.5 to 5 km in lengths, and order 50 to 250 m in breadths. Corresponding changes due to a projected sea level rise of 50 cm are: increases in both lengths of order 1 to 2.5 km and breadths of order 70 to 100 m. In both cases, the biggest changes will occur in larger estuaries.

Modelling

Conditions in the Mersey Estuary were investigated using a 3-D Eulerian fine-resolution hydrodynamic model coupled with a Lagrangian, random-walk sediment module. The model showed how the dominant fluxes involve fine (silt) sediments on spring tides. Model estimates of net imports of sediments agree with observed ranges for sediments of diameter of approximately 50 μm. and both dredging records and in situ observations indicate that sediments of this kind predominate. The model showed little influence of river flow, saline intrusion or channel

deepening on the sediment regime. Conversely, the net fluxes were sensitive to both the bed friction coefficient and the phase lag θ of elevation relative to velocity.

Upper-bound rates of infill of up to 10 Mt a^{-1} are indicated by the model, comparable with annual dredging rates of up to 5 Mt. The limited mobility of coarse sediments was contrasted with the near-continuously suspended nature of the finest clay. A sensible match between the net sedimentation rates indicated by the model and the net observed deposition rate was found to occur for silty sand corresponding directly with evidence from dredging records and from direct sampling. While the model indicated sedimentation rates might increase significantly for much finer particles, this is likely to be restricted by the limited availability of such material in the adjacent coastal zone.

The present approach can be readily extended to study changes in biological mediation of bottom sediments, impacts of waves, consolidation, and the interactions between mixed sediments.

7. CONCLUSIONS

We do not expect dramatic changes in UK estuarine responses to tides or surges from the projected impacts of Global Climate Change (GCC) over the next few decades. Some enhanced sensitivity might be found in relation to shorter 'period' (6 hr) surges associated with secondary depressions on the West Coast, particularly in larger estuaries. Likewise, maintaining fixed defences alongside continuous increases in mean sea level may enhance surge response in the shallowest estuaries.

There is no evidence from the present study that GCC will lead to dramatic changes in sediment regimes. In the absence of 'hard geology', enhanced river flows may result in increases in estuarine lengths and depths, though with the proportional increases less than half that of the change in river flow and developing over decades. The potential influence on effective sea-bed roughness of changing flora and fauna could, in some cases, have abrupt and dramatic impacts on dynamics and bathymetry.

Monitoring Strategies

The bathymetric surveys and tide gauge records used in this study are among the best data sets available anywhere spanning the past century. To provide confidence in any future predictions we need to use historic records and initiate ongoing monitoring. The present analyses of historic long-term intensive observations in the Mersey emphasises their value in addressing these issues.

A monitoring strategy for studying bathymetric changes, capable of better resolving processes operating in similar estuaries, should include the following:

(1) shore-based tide gauges throughout the length of the estuary, supplemented by water level recorders in the deeper channels;

(2) regular bathymetric surveys, e.g., 10-year intervals with more frequent re-surveying in regions of the estuary where low water channels are mobile; referencing of bathymetry data using differential Global Positioning System with levels verified against known local benchmarks;

(3) a network of moored platforms with instruments for measuring currents (e.g., vertical current profiles with ADCPs), waves, sediment concentrations, temperature and salinity.

Theoretical Frameworks

The recent success of new theories (Prandle *et al.*, 2005) in explaining of new theories in explaining evolution of morphologies over the 10000 years of Holocene adjustments lends confidence for their use in extrapolation over the next few decades.

Controlling mechanisms for the import/export of fine sediments depend critically on the phase lead of tidal currents relative to elevation. This phase lead also determines the net energy dissipation in estuaries. Hence the

stability of the overall tidal dynamics, the associated sediment regime and bathymetry are directly linked and hence bathymetries are likely to evolve slowly as indicated by the observed annual decrease in net volume in the Mersey.

Modelling

An accurate fine-resolution 3-D hydrodynamic module is essential. Uncertainties remain in the prescription of: sediment erosion and deposition, bed roughness and turbulence intensity, and structure (i.e., the overall near-bed boundary layer dynamics). The use of random-walk particle models to simulate sediment movements permits detailed tracking of sequences of sediment erosion, transport, and deposition. Such models are well suited to examining immediate changes associated with GCC such as in sea level, river flow, and sediment supply.

Modellers must recognise that the sort of observations required to rigorously assess progress in the development of sediment modules are unlikely to be available for the foreseeable future. Hence, as outlined here, models should be used for determining ensembles of possible outcomes. Here the model showed evidence of stabilising feedbacks that limit the ensemble spread anticipated from isolated tests of parameter ranges. The value of theoretical frameworks in interpreting the resulting, seemingly diverse, results has been shown. Likewise, model simulations and assessments must extend beyond the conventional short term comparison of suspended concentrations to include: spring-neap and seasonal variations, changing distributions of surficial sediments, and long term deposition rates derived from sequential bathymetric surveys. Clearer insights and understanding of scaling issues should emerge by comparing results from many such model applications, covering a range of estuaries, against the new theoretical frameworks and whatever observational data can be obtained.

REFERENCES

[1] Agar, M., McDowell, D.M., 1971. The Sea Approaches to the Port of Liverpool. Proceedings of the Institution of Civil Engineers 49, 145–156.

[2] Burgess, K.A., Balson, P., Dyer, K.R., Orford, J., Townend, I.H., 2002. FutureCoast–The Integration of Knowledge to Assess Future Coastal Evolution at a National Scale. Paper Presented at the 28th International Conference on Coastal Engineering. *American Society of Civil Engineering*, Vol. 3. ASCE, New York. pp. 3221–3233.

[3] Defra/Environment Agency, 2003. Climate Change Scenarios UKCIP02: Implementation for Flood and Coastal Defence. R & D Technical Summary W5B-029/TS.

[4] Defra/Environment Agency, 2004. Impact of Climate Change on Flood Flows in River Catchments. Technical Summary W5-032/TS.

[5] Dronkers, J., 1998. Morphodynamics of the Dutch delta. In: Dronkers, J., Scheffers, M. (Eds.), Physics of Estuaries and Coastal Seas. Proceedings of the 8th International Biennial Conference on Physics of Estuaries and Coastal Seas, The Hague, Netherlands, 9–12, September 1996. A.A. Balkema, Rotterdam, pp. 297–304.

[6] Fischer, H.B., List, E.J., Koh, R.C.Y., Imberger, J., Brooks, N.H., 1979. Mixing in Inland and Coastal Waters. New York, Academic Press. 483 pp.

[7] Friedrichs, C.T., Aubrey, D.G., 1998. Non-linear Tidal Distortion in Shallow Well-Mixed Estuaries: A Synthesis. Estuarine, Coastal and Shelf Science 27 (5), 521–545.

[8] Hill, D.C., Jones, S.E., Prandle, D., 2003. Dervivation of Sediment Resuspension Rates from Acoustic Backscatter Time-series in Tidal Waters. Continental Shelf Research 23(1), 19–40, doi:10.1016/S0278-4343(02)00170-X.

[9] Hutchinson, S.M., Prandle, D., 1994. Siltation in the saltmarsh of the Dee Estuary derived from ^{137}Cs analysis of shallow cores. Estuarine, Coastal and Shelf Science 38(5), 471–478.

[10] IPCC, 2001. Climate Change 2001. Synthesis Report. A Contribution of Working Groups I, II, and III to the Third Assessment Report of the Intergovernmental Panel on Climate Change [Watson, R.T. and the Core Writing Team (eds.)]. Cambridge University Press, Cambridge, United Kingdom, and New York, NY, USA, 398 pp.

[11] Lane, A., 2004. Bathymetric evolution of the Mersey Estuary, UK, 1906–1997: causes and effects. Estuarine, Coastal and Shelf Science 59(2), 249–263, doi:10.1016/j.ecss. 2003.09.003.

[12] Lane, A., Prandle, D., 2006. Random-walk Particle Modelling for Estimating Bathymetric Evolution of an Estuary. Estuarine, Coastal and Shelf Science, 68(1–2), 175–187, doi:10.1016/j.ecss.2006.01.016.

[13] Lane, A., Prandle, D., Harrison, A.J., Jones, P.D., Jarvis, C.J., 1997. Measuring Fluxes in Estuaries: Sensitivity to Instrumentation and Associated Data Analyses. Estuarine, Coastal and Shelf Science 45(4), 433–451, doi:10.1006/ecss.1996.0220.

[14] Prandle, D., 1982. The Vertical Structure of Tidal Currents and other Oscillatory Flows. Continental Shelf Research, 1(2), 191–207, doi:10.1016/0278-4343(82)90004-8.

[15] Prandle, D., 1989. The Impact of Mean Sea level change on Estuarine Dynamics Proceedings of the 13th Congress of the IAHR, Ottawa, Canada.

[16] Prandle, D., 1997. Tidal Characteristics of Suspended Sediment Concentrations. ASCE, *Journal of Hydraulic Engineering,* 123(4), 341–350, doi:10.1061/(ASCE)0733-9429(1997)123: 4(341).

[17] Prandle, D., 2003. Relationships Between Tidal Dynamics and Bathymetry in Strongly Convergent Estuaries. *Journal of Physical Oceanography*, 33, 2738–2750.

[18] Prandle, D., 2004a. How tides and River Flows Determine Estuarine Bathymetries. Progress in Oceanography, 61, 1–26, doi:10.1016/j.pocean.2004.03.001.

[19] Prandle, D., 2004b. Sediment Trapping, Turbidity Maxima, and Bathymetric Stability in Macrotidal Estuaries. *Journal of Geophysical Research*, 109, C08001, 13pp., doi:10.1029/2004JC002271.

[20] Prandle, D., 2004c. Saline Intrusion in Partially Mixed Estuaries. Estuarine, Coastal and Shelf Science, 59(3), 385–397, doi:10.1016/j.ecss.2003.10.001.

[21] Prandle, D., 2006. Dynamical Controls on Estuarine Bathymetries: Assessment against UK Database. Estuarine, Coastal and Shelf Science, 68(1–2), 282–288, doi:10.1016/j.ecss.2006.02.009.

[22] Prandle, D., Lane, A., Manning, A.J., 2005, Estuaries are not so Unique. Geophysical Research Letters, 32, L23614, doi:10.1029/2005GL024797.

[23] Prandle, D., Lane, A., Manning, A.J., 2006, New Typologies for Estuarine Morphology. Geomorphology, 81(3-4), 309-315, doi:10.1016/j.geomorph.2006.04.017.

[24] Prandle, D., Murray, A., Johnson, R., 1990. Analyses of Flux Measurements in the River Mersey. pp. 413–430 in: Residual Currents and Long Term Transport, Coastal and Estuarine Studies, 38, Cheng, R.T. (Ed.), Springer-Verlag, New York, 544 pp.

[25] Prandle, D., Rahman, M., 1980. Tidal Response in Estuaries. *Journal of Physical Oceanography*, 10(10), 1522–1573.

[26] Price, W.A., Kendrick, M.P., 1963. Field and Model Investigation into the Reasons for Siltation in the Mersey Estuary. Proceedings of the Institute of Civil Engineers 24, 473–517.

[27] Simpson, J.H., Hunter, J.R., 1974. Fronts in the Irish Sea. Nature, 250, 404–406.

[28] Thomas, C.G., Spearman, J.R., Turnbull, M.J., 2002. Historical Morphological Change in the Mersey Estuary, Continental Shelf Research, 22(11–13), 1775–1794, doi:10.1016/S0278-4343(02)00037-7.

[29] Woodworth, P.L., Tsimplis, M.N., Flather, R.A., Shennan, I., 1999. A Review of the Trends Observed in British Isles Mean Sea level Data Measured by tide Gauges. *Geophysical Journal International*, 136(3), 651–670.

Andrew Lane
Proudman Oceanographic Laboratory, Joseph Proudman Building
6 Brownlow Street, Liverpool L3 5DA, UK

David Prandle
Department of Earth and Ocean Sciences, University of Liverpool
4 Brownlow Street, Liverpool L69 3GP, UK